Vol. 48: 139–154, 2022
https://doi.org/10.3354/esr01193

ENDANGERED SPECIES RESEARCH
Endang Species Res

Published July 21

Investigating the thermal physiology of Critically Endangered North Atlantic right whales *Eubalaena glacialis* via aerial infrared thermography

Gina L. Lonati[1,*], Daniel P. Zitterbart[2], Carolyn A. Miller[3], Peter Corkeron[4], Christin T. Murphy[5], Michael J. Moore[6]

[1]University of New Brunswick Saint John, Department of Biological Sciences, New Brunswick E2L 4L5, Canada
[2]Applied Ocean Physics and Engineering Department, Woods Hole Oceanographic Institution, Woods Hole, MA 02543, USA
[3]Marine Chemistry and Geochemistry Department, Woods Hole Oceanographic Institution, Woods Hole, MA 02543, USA
[4]Anderson Cabot Center for Ocean Life at the New England Aquarium, Boston, MA 02110, USA
[5]Bio-Inspired Research and Development Laboratory, Naval Undersea Warfare Center Division Newport, Newport, RI 02841, USA
[6]Biology Department, Woods Hole Oceanographic Institution, Woods Hole, MA 02543, USA

ABSTRACT: The Critically Endangered status of North Atlantic right whales *Eubalaena glacialis* (NARWs) warrants the development of new, less invasive technology to monitor the health of individuals. Combined with advancements in remotely piloted aircraft systems (RPAS, commonly 'drones'), infrared thermography (IRT) is being increasingly used to detect and count marine mammals and study their physiology. We conducted RPAS-based IRT over NARWs in Cape Cod Bay, MA, USA, in 2017 and 2018. Observations demonstrated 3 particularly useful applications of RPAS-based IRT to study large whales: (1) exploring patterns of cranial heat loss and providing insight into the physiological mechanisms that produce these patterns; (2) tracking subsurface individuals in real-time (depending on the thermal stratification of the water column) using cold surface water anomalies resulting from fluke upstrokes; and (3) detecting natural changes in superficial blood circulation or diagnosing pathology based on heat anomalies on post-cranial body surfaces. These qualitative applications present a new, important opportunity to study, monitor, and conserve large whales, particularly rare and at-risk species such as NARWs. Despite the challenges of using this technology in aquatic environments, the applications of RPAS-based IRT for monitoring the health and behavior of endangered marine mammals, including the collection of quantitative data on thermal physiology, will continue to diversify.

KEY WORDS: Cetaceans · Drone · Health · Marine mammals · Remote sensing · Temperature · UAVs

1. INTRODUCTION

1.1. North Atlantic right whales and population monitoring

The North Atlantic right whale *Eubalaena glacialis* (NARW) is a large, Critically Endangered mysticete whale that primarily inhabits the northwest Atlantic Ocean (Cooke 2020). These whales forage on small plankton prey (primarily calanoid copepods) in the spring, summer, and early fall off the Atlantic coast of southeastern Canada and the northeastern USA. In the winter, portions of the population undergo fasting migrations to waters off the southeast coast of the USA, where adult females give birth to calves. NARWs were nearly extirpated due to whaling between the 18th and 20th centuries (Harcourt et al. 2019). At the end of 2020, the best estimate of population size was still only 336 individuals, with fewer than 100 known reproductively active females (Moore et al. 2021, Pettis et al. 2022).

*Corresponding author: gina.lonati@unb.ca

Publisher: Inter-Research · www.int-res.com

The recovery of NARWs has been hampered by persistent human impacts (namely entanglements in fishing gear and collisions with vessels) as well as decreases in the quality and quantity of their copepod prey due to climate change (Knowlton & Kraus 2001, Meyer-Gutbrod et al. 2015, 2021, Record et al. 2019, Sharp et al. 2019, Moore et al. 2021). As a result, mortalities have increased and reproductive rates have declined, while the health of individual whales has also deteriorated (Rolland et al. 2016, Sharp et al. 2019, Moore et al. 2021). For example, NARWs are in significantly poorer body condition than other members of their genus, *Eubalaena* (includes southern, North Pacific, and North Atlantic right whales) (Miller et al. 2011, Christiansen et al. 2020). Now more than ever, it is crucial that we develop more effective ways to monitor individual health in order to gain a more comprehensive understanding of overall population health, especially as more drastic management efforts are being implemented (Davies & Brillant 2019). However, assessing the health of individual large whales is inherently challenging because live capture is unsafe or impractical, individuals cannot be evaluated in managed care, and NARWs range over vast distances.

1.2. Infrared thermography and remotely piloted aircraft systems

Infrared thermography (IRT) is the use of contactless sensors to measure the thermal radiation emitted from objects. Thermographic cameras translate measurements of radiation into intensity-coded thermographic images for easier interpretation of radiated heat patterns. Originally developed for military purposes, IRT is now commonly used for nighttime surveillance, medical testing, and infrastructure inspections, but it is also a valuable tool for studying the thermal physiology of ectotherms and endotherms (reviewed in McCafferty 2007, Cilulko et al. 2013, Lathlean & Seuront 2014, Tattersall 2016). It has also gained popularity in veterinary medicine, because it can illuminate changes in peripheral blood flow; for example, abnormal or asymmetrical patterns of peripheral heat could indicate inflammation, infection, stress, or even pregnancy in livestock and terrestrial wildlife (reviewed in Knížková et al. 2007, McCafferty 2007, Cilulko et al. 2013, Nääs et al. 2014, Rekant et al. 2016). Because IRT relies on naturally emitted radiation and does not require the manipulation of animals, it can be much more practical than invasive methods, such as thermal telemetry via ingested radio pills (e.g. Mackay 1964, Cutchis et al. 1988, Austin et al. 2006), archival tag devices (Westgate et al. 2007), or direct insertion of oral or rectal thermometers (Katsumata et al. 2006, McCafferty et al. 2015, Martony et al. 2020). Thus, IRT has clear advantages for studying species in natural, undisturbed states, especially cryptic or endangered species for which more invasive methods are infeasible or impermissible. It is important to note, however, that IRT only permits surface or peripheral measurements (Tattersall 2016), which are not always representative of internal temperatures (McCafferty et al. 2015). Furthermore, thermal radiation attenuates quickly in water, so submerged body areas cannot be sampled.

Long-wave IRT (8–14 µm wavelength) is becoming a popular tool for the detection of marine mammals (reviewed in Lathlean & Seuront 2014), based on apparent temperature differentials that exist between an animal's skin or exhaled breath and its surroundings (Cuyler et al. 1992, Barbieri et al. 2009). Conveniently, thermal sensors can be placed on a variety of platforms for different detection purposes. Land-based IRT has been used to detect and count the blows of nearshore gray whales *Eschrichitus robustus* to quantify migration rates (Perryman et al. 1999), as well as record the foraging activity of Steller sea lions *Eumetopias jubatus* (Thomas & Thorne 2001). Vessel-based IRT could reduce the risk of collision or excessive noise exposure by detecting whales and their blows in low-light conditions (Yonehara et al. 2012, Zitterbart et al. 2013, 2020, Horton et al. 2017). Aerial IRT via planes and remotely piloted aircraft systems (RPAS, or commonly 'drones') has been used to supplement visual counts of pinnipeds (Lydersen et al. 2012, Seymour et al. 2017, Johnston et al. 2017) and polar bear *Ursus maritimus* dens (York et al. 2004), often making detections that are overlooked by visual observers in real-time. In the case of ringed seals *Pusa hispida* in the Canadian Arctic, density estimates that included aerial IRT detections were approximately 2–3 times greater than estimates produced by analyses of visual observer counts alone (Young et al. 2019).

Other researchers have begun using IRT to study aspects of marine mammal thermal physiology (reviewed in Lathlean & Seuront 2014). In particular, studies on stranded, amphibious, and captive marine mammals have led to a better understanding of heat dissipation, thermal windows, and other aspects of thermal physiology in pinnipeds (e.g. Dehnhardt et al. 1998, Mauck et al. 2003, Nienaber et al. 2010, Erdsack et al. 2012, 2014, Codde et al. 2016, Guerrero et

al. 2021), dolphins (Williams et al. 1999, Mauck et al. 2000, Pabst et al. 2002, Barbieri et al. 2009), and mysticete whales (Heyning 2001, Ford et al. 2013). A recent study (Horton et al. 2019) used RPAS-based IRT to successfully capture thermographs of a mother and calf humpback whale *Megaptera novaeangliae*. Analysis of the heat anomalies observed on the mother's dorsal fin supported the use of RPAS-based IRT to remotely measure large whale heart rates under certain conditions. Additionally, close-range IRT of the blowholes of small, captive bottlenose dolphins *Tursiops truncatus* and beluga whales *Delphinapterus leucas* yielded values which were within 1°C of rectal temperatures (Melero et al. 2015), supporting that IRT of the blowholes of free-ranging cetaceans could be used to estimate internal body temperature.

1.3. Objectives

With the impacts of anthropogenic stressors increasing and the NARW population declining, there is a clear need for improved health monitoring tools for these large whales. Most management decisions rely on population-level health metrics, such as annual mortalities, reproductive rates, and reports of sublethal injuries, to gauge conservation success. However, individual health metrics, such as body condition, heart rate, hormone and contaminant levels, and others, would provide a more detailed perspective of the impacts of multiple stressors on these whales (Nowacek et al. 2016, Pirotta et al. 2018, 2022, Moore et al. 2021). Vital rates are difficult to obtain from animals without hands-on health assessments, so developing innovative methodologies that can measure behavioral or physiological indicators of health while causing minimal disturbance to the whale is critical (Moore et al. 2021). As thermal physiology is strongly linked with the energetics and health of animals, RPAS-based IRT could be a useful tool for non-invasively monitoring the responses of large whales to multiple stressors. However, it is essential to conduct baseline IRT observations of whales before informed interpretations of health can be made with these data.

Thus, the goal of this study was to outline several ways in which RPAS-based IRT can be used to investigate the thermal physiology and health of Critically Endangered NARWs. Using relative temperature data obtained from RPAS-based IRT of NARWs in Cape Cod Bay, MA, USA, supplemented by studies of rostral tissue collected from a deceased NARW, we specifically demonstrate the following applications: (1) exploring patterns of cranial heat loss and the anatomical structures potentially responsible for these patterns; (2) tracking whales in real-time by observing thermal 'flukeprints', i.e. cooler subsurface water that upwells from depth during a fluke upstroke (Churnside et al. 2009, Levy et al. 2011, Florko et al. 2021); and (3) using post-cranial heat anomalies to diagnose pathology or detect other changes in peripheral blood flow. We consider how the technology can improve our ability to evaluate large whale health, particularly for NARWs in the face of human impacts, while also acknowledging the myriad challenges and limitations related to the use of RPAS-based IRT in aquatic environments.

2. MATERIALS AND METHODS

2.1. RPAS flights

RPAS research was conducted as part of a larger research program on the health of NARWs *Eubalaena glacialis* in Cape Cod Bay. Fieldwork was conducted between the months of March and May in 2017 and 2018 (Table 1). A DJI Inspire 1 RPAS (weight: 3119 g including battery) was equipped with a Zenmuse XT 'Advanced Radiometry' forward-looking infrared camera (FLIR Systems; weight: 270 g; resolution: 640 × 512 pixels; frame rate: 30 Hz; focal length: 13 mm) that captured non-radiometric thermal videos (i.e. sequences of thermographic images with pixels false color-coded by relative temperatures in MP4 format). Videos allowed us to visualize the entire surfacing of a whale, including complete respiratory cycles, versus timed still images. However, the non-radiometric metadata from these videos only provided qualitative thermal differentials, as opposed to absolute measurements of temperatures. An Apple iPad Air 2 running DJI Go (version 3.1.26) was used to pilot the RPAS, control the Zenmuse XT

Table 1. Summary of flights with the DJI Inspire 1 over North Atlantic right whales in Cape Cod Bay, MA, USA

Dates	Total flights	Average ± SD flight time (min)	Total flight time (h)
27 April 2017	3	11.63 ± 0.91	0.58
29 March 2018	4	9.91 ± 1.11	0.66
27 April 2018	7	8.82 ± 2.55	1.03
28 April 2018	3	10.86 ± 1.45	0.54
06 May 2018	5	8.60 ± 3.62	0.72
Total	22	9.63 ± 2.47	3.53

gimbal, and view live-stream thermal video from the Zenmuse XT. In addition, a GoPro HERO3 (weight: 77 g including battery; resolution: 1920 × 1080 pixels; frame rate: 30 Hz) was attached with self-adhesive tapes (3M Dual Lock Reclosable Fasteners) to the underside of the RPAS to obtain simultaneous RGB (i.e. visible spectrum) video in MP4 format (Fig. 1). The total take-off weight of the RPAS system was 3596 g.

The RPAS was hand-launched and hand-caught from a 17.5 m long research vessel when winds were <13 knots, Beaufort sea state was ≤3, visibility was >5 km, and there was no precipitation. A 2-person team operated the RPAS: a pilot responsible for navigating the RPAS and a co-pilot who monitored the battery level, captured imagery, and assisted with directing the pilot using a secondary remote controller. Barometric altitude was recorded by the RPAS. When whales were located, the RPAS approached overhead at a maximum altitude of 81 m before descending vertically to a minimum of 3 m with the cameras approximately nadir for close observations of the head and blowholes, prior to collecting blow samples for another study. GoPro videos started before launch and ended upon landing. Thermal videos were triggered via the DJI Go app when the RPAS was approaching and overhead whales. The RPAS returned to the vessel when the battery reached ~30% of full charge. The average (±SD) flight time was 9.6 ± 2.5 min, with a maximum of 12.4 min. The pilot and an additional crew member visually monitored whales for disturbance behaviors (e.g. interrupted surfacings, abbreviated or abnormal respirations, sinking without fluking, frequent reorientations away from RPAS, and turning while fluking) during flights.

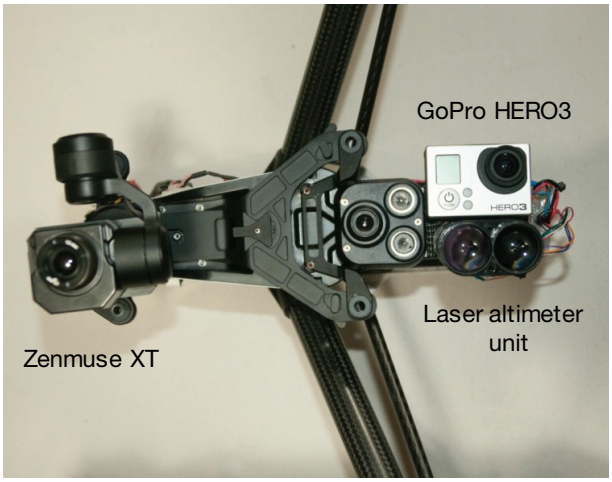

Fig. 1. Underside of the DJI Inspire 1 remotely piloted aircraft system (RPAS), showing the configuration of the gimballed Zenmuse XT, the GoPro HERO3, and a custom-mounted laser altimeter unit, used for a separate parallel study. Note that the GoPro was not gimballed and therefore often oriented differently than the Zenmuse XT. The laser altimeter malfunctioned during some of the flights for this study, so we used the RPAS's barometric altitudes instead. The front of the RPAS is to the left

2.2. RPAS image analyses

Based on previous research (Melero et al. 2015, Horton et al. 2019), open blowholes appear as heat anomalies relative to surface water temperatures during respirations. Because thermal and RGB videos were not necessarily time-aligned for all flights, thermal video frames from the Zenmuse XT were manually aligned with RGB video frames from the GoPro based on the timing of blowholes opening and closing. Frame alignments were confirmed through the synchronicity of other heat anomalies, such as birds present in the field of view or other body parts (e.g. the flukes) breaking the surface of the water. We then qualitatively reviewed the non-radiometric thermal videos and RGB videos from each whale encounter and identified any additional heat anomalies over areas of the body that emerged during a surfacing, as well as cold anomalies associated with fluke upstrokes of whales (i.e. thermal flukeprints). RGB imagery was also sent to the Anderson Cabot Center for Ocean Life at the New England Aquarium to photo-identify NARWs that were observed.

2.3. Callosity dissection and warming studies

To investigate the potential source of heat observed in thermographs of NARW heads, we conducted 2 studies using some rostral tissue collected during the necropsy of a 12.6 m long, moderately decomposed, male NARW (GA2006-025Eg; Catalog ID 3508). The tissue sample, which measured 128 × 35 × ~6 cm thick, was collected under NOAA permit 932-1489 and stored frozen at −20°C before being examined for these 2 studies.

Dilated peripheral blood vessels could heat the skin surface through conduction, producing the heat observed in overhead thermographs, so the purpose of the first tissue study was to describe the sample's superficial vasculature and measure its thickness. First, we coronally cross-sectioned the rostral tissue in 4 locations (Fig. 2A) and collected 2 histology sam-

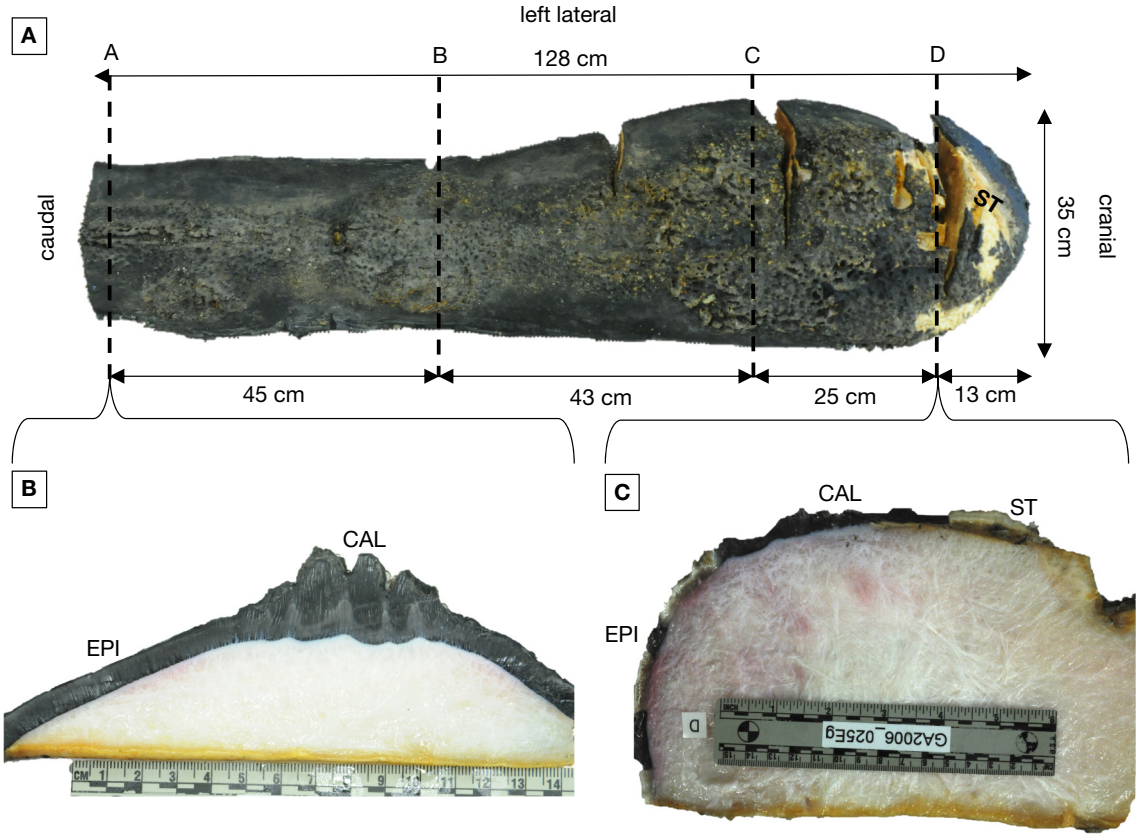

Fig. 2. Dissection of rostral tissue from a North Atlantic right whale (GA2006-025Eg; Catalog ID 3508). (A) Dorsal view of the rostral tissue showing where the 4 cross-sections were located for histological sampling. Note that the pre-existing incisions seen in A were part of a series of propeller slices that were the proximate cause of death. (B) Cross-section A (most caudal cross-section), showing the difference in thickness between the epidermis (EPI) and keratinized callosity (CAL). (C) Cross-section D (most cranial cross-section), which had some scar tissue (ST) present on the dorsal and left lateral aspects. Thicknesses of the callosities and epidermis from all cross-sections are summarized in Table 3

ples within each cross-section (Fig. 2B). One sample included the dorsal callosity — a raised area of thickened, keratinized tissue that characterizes members of the genus *Eubalaena*. Shortly after birth, these callosities become pitted and colonized by barnacles and cyamid crustaceans (Reeb et al. 2007). Each NARW has a unique callosity pattern, so they are used to photo-identify individual whales. The second sample included only left lateral epidermis, except in cross-section D, where some scarred callosity was also included (Fig. 2C). We measured the thickness of the epidermis and the minimum and maximum thicknesses of the callosity along each coronal cross-section to the nearest 0.1 cm. The rostral tissue was then returned to the −20°C freezer before the warming study (see below). Histological samples were fixed in 10% neutral-buffered formalin, routinely processed into paraffin, and stained with hematoxylin and eosin. We then examined the tissues under the microscope for the presence of arteriovenous anastomoses (AVAs) and countercurrent arrangement of arteries and veins comparable to those described by Elsner et al. (2004) in the bowhead whale *Balaena mysticetus*, that could act as an internal source of heat radiating up through the rostral epithelium.

Alternatively, differential warming of tissues exposed to air and solar radiation during skim feeding could influence heat patterns observed in overhead thermographs, so the purpose of the second study was to investigate the thermal inertia (the slowness with which an object's temperature reaches that of its environment) of different parts of the rostrum. We began by re-thawing the rostral tissue from GA2006-025Eg overnight at room temperature (approximately 19.6°C). NARW epidermis and dermis are relatively resistant to decomposition when compared to muscle, viscera, and brain (M. Moore, pers. obs.), and there was no gross evidence of decomposition during the thawing process. The following morning, we moved the tissue to a chiller at 4.9°C. After 4 h, we removed the tissue from the

chiller and recorded surface temperatures of the callosity and adjacent epithelium with a single thermistor (Fluke 87 True RMS multimeter, 80TK thermocouple and Fluke 80PK-22 SureGrip Immersion Temperature Probe) as the tissue was exposed to room temperature for 20 min (an approximate duration of a bout of skim feeding behavior in NARWs and the maximum time the rostrum might be continuously exposed to air; M. Moore, pers. obs.). We allowed the thermistor to equilibrate to the callosity or epithelium adjacent to the callosity (hereafter, 'peri-callosity epithelium') for approximately 1 min prior to recording each temperature. Generalized linear models with subsequent AIC analysis (in R; R Core Team 2021) were used to evaluate the warming rates of the 2 tissues. Given the heterogeneous heat signatures observed in thermographs of NARW heads (see Section 3.2), we would expect the warming rates of the callosity and epithelium to be significantly different if air temperature or solar radiation was responsible for these signatures.

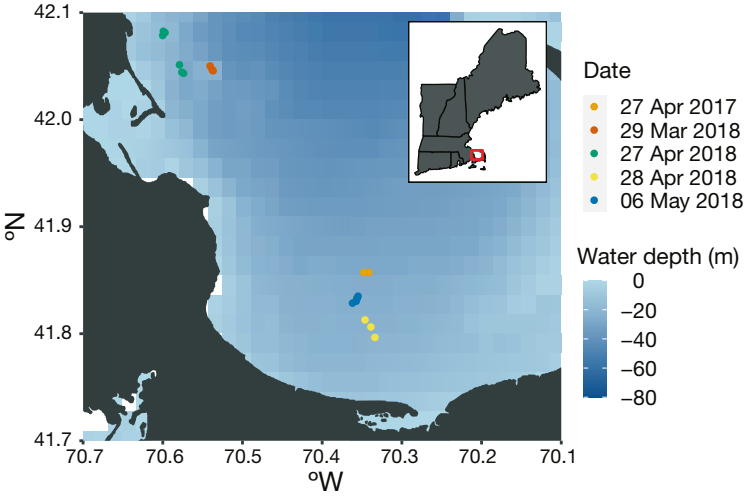

Fig. 3. Launch locations of the remotely piloted aircraft system in Cape Cod Bay, MA, USA in 2017 and 2018, color-coded by day

3. RESULTS

3.1. RPAS flights

A total of 22 flights with the IRT camera were conducted over traveling and feeding NARWs *Eubalaena glacialis* in Cape Cod Bay, for a total of 3.5 h of flight time over 5 separate field days in 2017 and 2018 (Table 1, Fig. 3). We did not observe any of the aforementioned disturbance behaviors from NARWs during RPAS flights. We obtained 26 thermal videos (MP4) of 16 unique NARWs (Identification Database of the North Atlantic Right Whale Consortium). This included 80 total respirations, with an average of 5 respirations (range: 1–18 respirations) per individual (Table 2).

3.2. Rostral heat

As expected, when blowholes were open during respiration, they appeared as distinct heat anomalies compared to the water surface (Fig. 4A,B, Video S1 in the Supplement at www.int-res.com/articles/suppl/n048p139_supp/). Furthermore, NARWs exhibited unique patterns of heat radiating from their rostra upon surfacing and during skim-feeding (Fig. 4, Video S1). Specifically, epithelial surfaces adjacent to the keratinized callosities radiated more heat than the callosities and the post-cranial epithelium. Cooler epithelium between the warmer peri-callosity epithelium and the waterline at the time of the image is evident in Fig. 4. We also observed heat anomalies at the tips of the rostra of some NARWs during skim feeding (Fig. 5).

Histological examination of rostral tissue demonstrated that neither the callosities (dorsal rostrum) nor the epithelial tissue (left lateral rostrum) exhibited any major underlying vasculature, such as countercurrent or AVA vessels (Fig. 6). To quantify the amount of insulative tissue mass on the dorsal rostrum, thicknesses of callosities and epidermis along the 4 coronal cross-sections are summarized in Table 3.

By the time we started recording temperatures for the warming study, the surfaces of the callosity and

Table 2. Summary of North Atlantic right whale demographics based on photo-identified individuals (n = 16) from remotely piloted aircraft system imagery (Identification Database of the North Atlantic Right Whale Consortium). IRT: infrared thermography

Demographic group	Total individuals	Total respiratory events observed via IRT
Males <10 yr old	3	12
Males >10 yr old	5	31
Non-reproductive females	5	29
Reproductive females	3[a]	8
Total	16	80

[a]One reproductive female was observed with a newborn calf 8 mo after field observations, meaning she was likely pregnant during observations. See Section 3.5 and Fig. 10

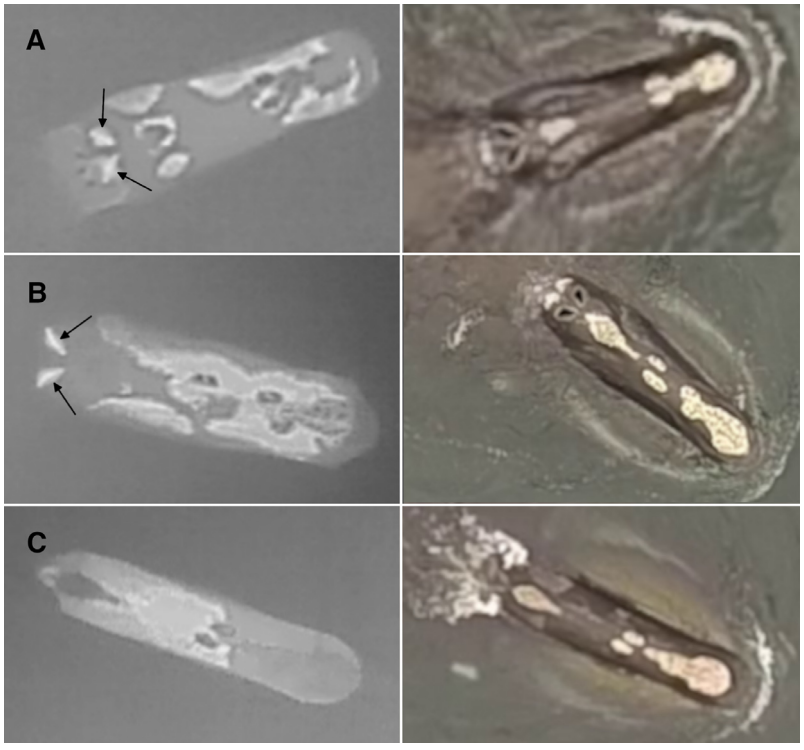

Fig. 4. Time-aligned video frames from the Zenmuse XT (left, white-hot color palette) and the GoPro HERO3 (right), demonstrating the heat loss patterns relative to the callosities on the rostra of 3 unique North Atlantic right whales. Specifically, the peri-callosity epithelium exuded more heat than the keratinized callosities. Black arrows in A and B highlight the heat anomalies from open blowholes during respirations. Blowholes were closed in C. The whale in A was a 3-yr-old male (Catalog ID 4523), and the whales in panels B and C were both females (Catalog IDs 4540 and 3908), ages 5 and 9 yr old, respectively (Identification Database of the North Atlantic Right Whale Consortium)

peri-callosity epithelium were 8.7 and 9.7°C, respectively. The interaction between elapsed time and tissue type was not significant ($p = 0.915$), meaning that the rates at which both tissue surfaces warmed were not significantly different (Fig. 7). The most parsimonious model was an additive one that included both elapsed time and tissue type ($F_{2,20} = 98.6$, $p < 0.01$, $r^2 = 0.9079$), indicating that both tissue surfaces warmed over time (at approximately 0.25°C min^{-1}), but that the peri-callosity epithelium remained warmer than the callosity for the 20 min of the study.

3.3. Thermal flukeprints

Cold anomalies associated with subsurface fluke strokes were observed on some days, allowing us to track whales more easily with the RPAS when they were underwater and not visible from the research vessel. Specifically, the thermal contrast between whale flukeprints and the surrounding water surface was greatest on 27 April 2017 and 28 April 2018 (Fig. 8, Video S2) and moderate on 27 April 2018. These days were characterized by low winds (≤10 knots), calm sea state (Beaufort ≤1, wave heights ≤0.1 m), and clear skies during flights. While local water temperatures were not recorded during flights, a temperature–depth profile collected for a separate research program in Cape Cod Bay (by the Massachusetts Water Resources Authority) during the week prior to 27 April 2017 suggests that the high-contrast thermal flukeprints corresponded with a thermocline in the upper ~5 m of the water column (Fig. 9). In addition, close-up thermographs of the heads of some skim-feeding NARWs showed cold-water anomalies around the whales' gapes on these days (Video S2).

Meanwhile, there was little to no thermal contrast between whale flukeprints and the surrounding water on

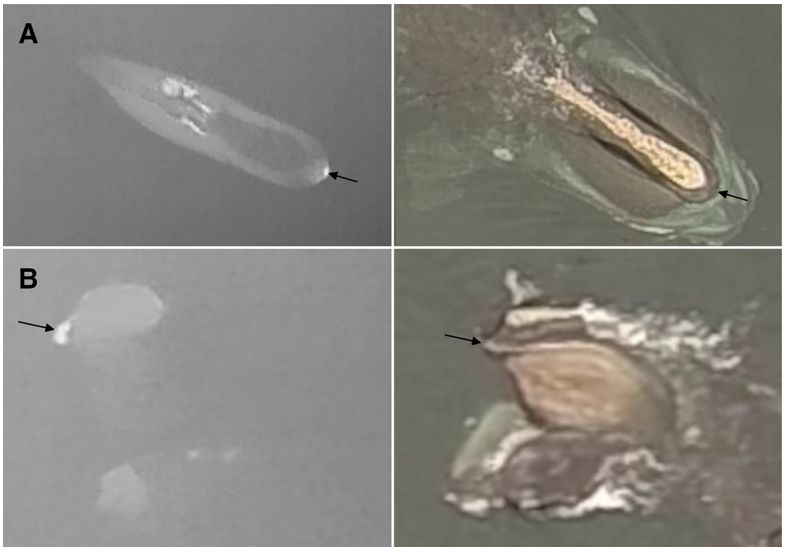

Fig. 5. Heat anomalies, as indicated by the black arrows, at the tips of the rostra of 2 different North Atlantic right whales observed while the whales were (A) skim-feeding (12-yr-old male; Catalog ID 3629) or (B) rolling left side up during skim-feeding at the surface (>36-yr-old female; Catalog ID 1425)

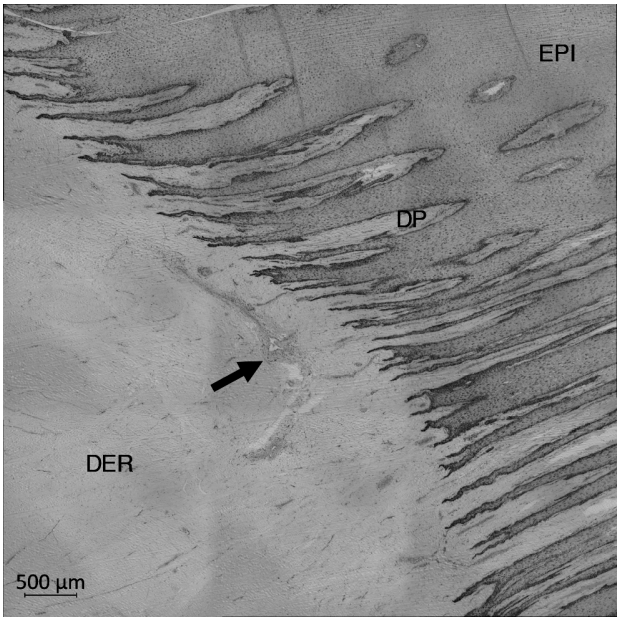

Fig. 6. Histological sample from the rostral tissue of a North Atlantic right whale (GA2006-025Eg; Catalog ID 3508), specifically the callosity at cross-section A (see Fig. 2A,B), demonstrating a lack of major vasculature underlying the epithelium and callosities. The black arrow indicates a single vein with no arteriovenous anastomoses or countercurrent specialization. DER: dermis; DP: dermal papillae; EPI: epidermis

29 March and 06 May 2018. Another temperature–depth profile from the week prior to 29 March 2018 did not exhibit a thermocline in the upper water column (Fig. 9; Massachusetts Water Resources Authority).

3.4. Post-cranial heat anomalies

One NARW observed during a flight on 28 April 2018 (at 41.8064°N, 70.3375°W) exhibited an anomalous heat signature on its dorsum (Fig. 10, Video S3).

Table 3. Thicknesses of callosities and epidermis from cross-sections depicted in Fig. 2. Note that all measurements of the epidermis were taken on the left lateral aspect of the callosities from this North Atlantic right whale (GA2006-025Eg; Catalog ID 3508)

Cross-section	Thickness of epidermis (cm)	Minimum thickness of callosity (cm)	Maximum thickness of callosity (cm)
A	0.8	0.9	2.9
B	0.7	0.9	1.7
C	0.7	0.8	2.8
D	0.6[a]	0.9	1.8
Average ± SD	0.7 ± 0.1	0.9 ± 0.1	2.3 ± 0.6

[a]Scar tissue included in measurement, see Fig. 2

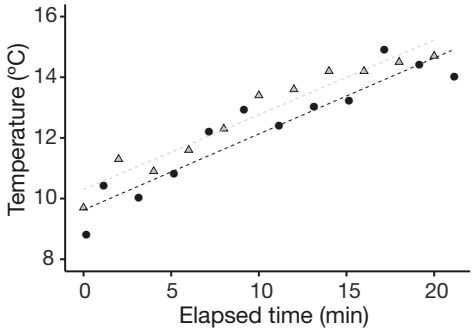

Fig. 7. Warming study data: surface temperature of the callosity (black circles) and adjacent epithelial tissue (gray triangles) over 20 min, after the rostral tissue from GA2006-025Eg (Catalog ID 3508) was removed from a 4.9°C chiller and exposed to room temperature (~19.6°C). The regressions (dashed lines) represent generalized linear models fit separately to each tissue ($F_{2,20}$ = 98.6, p < 0.01, r^2 = 0.9079)

Specifically, there was a small, ovoid patch of moderate heat exuding from the mid-dorsum (not visible in Fig. 10, see Video S3) as well as a large, rather diffuse patch of heat exuding from the dorsal lumbar

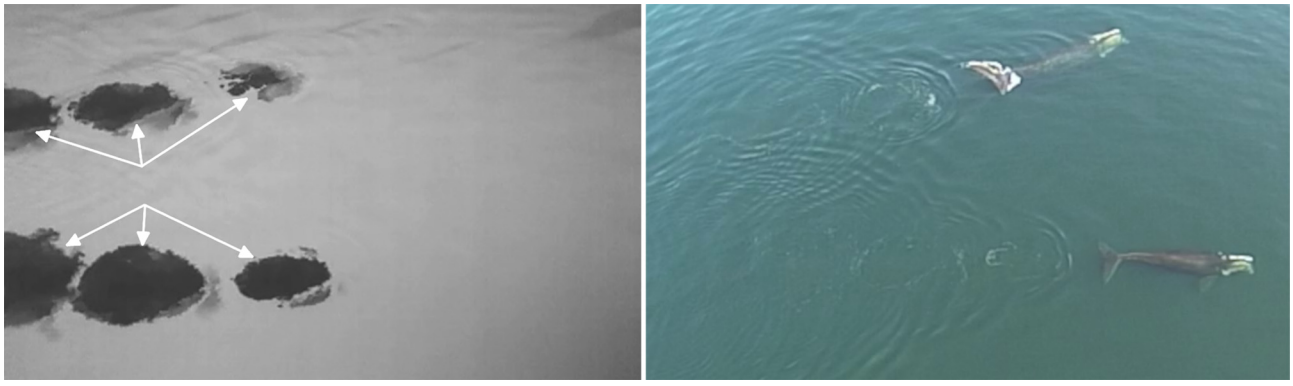

Fig. 8. Time-aligned video frames from the Zenmuse XT (left, white-hot color palette) and the GoPro HERO3 (right), demonstrating the cool thermal flukeprints, indicated by white arrows, that were generated during fluke upstrokes from 2 traveling North Atlantic right whales on 28 April 2018

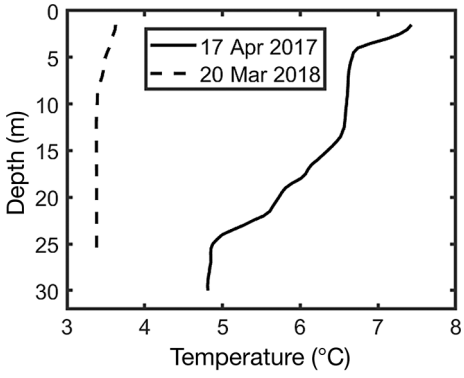

Fig. 9. Temperature–depth profiles from the upper water column in Cape Cod Bay, MA, USA, collected by the Massachusetts Water Resources Authority. Data from 17 April 2017 at 41.908167°N, 70.228333°W (solid line) demonstrate a thermocline in the top 5 m of the water column; we observed high-contrast thermal flukeprints produced by whales 10 d later, on 27 April 2017. The thermocline is not evident in the profile from 20 March 2018 at 41.850833°N, 70.453333°W (dashed line); thermal flukeprints were not apparent during flights 9 d later, on 29 March 2018

region. The heat was detected in the same location upon several consecutive surfacings and was especially apparent ~1–3 s after the dorsum emerged from the water (presumably once the thin layer of water was shed from the whale's back). Such heat was not observed on the dorsa of any other NARW in our study. Based on the RGB imagery obtained during flight, this individual was identified as NARW Catalog ID 2791, a reproductively active female that was observed 8 mo later with a newborn calf in Florida (Identification Database of the North Atlantic Right Whale Consortium).

4. DISCUSSION

RPAS-based IRT can provide novel insights into the thermal physiology of large whales. These insights are important for monitoring and better understanding the health of at-risk species, such as Critically Endangered NARWs. More specifically, documenting the baseline (i.e. nonpathological) envelope of NARW thermal signatures will aid in the identification and interpretation of anomalous signatures from whales in poor health or from whales experiencing other physiological phenomena (e.g. pregnancy). The RPAS platform offers a unique overhead and up-close perspective to particularly observe heat patterns from the dorsal head, track whales traveling subsurface in a stratified water column, and detect heat anomalies on the dorsal back. There are challenges and limitations, however, to interpreting data collected via aerial IRT in aquatic environments; these factors must be considered to improve future studies and develop new uses for monitoring the health of these whales.

4.1. Rostral heat

Obtaining thermographs of NARW heads allowed us to document the unique patterns of cranial heat loss in this species. Specifically, the epithelium around the callosities radiated more heat than other epithelial surfaces of the rostrum (Fig. 4). These patterns were visible on all field days, upon the first surfacing of whales after dives, and throughout bouts of surface skim-feeding. Thus, we do not believe these observations are an artifact of external phenomena related to the physics of IRT (see more below), but rather an indicator of inherent physiological processes.

To better understand the physiological mechanisms underlying the cranial heat signatures observed, we histologically examined rostral tissue from one necropsied NARW. In general, the dermis and hypodermis of cetaceans exhibit significant vascularization, likely for the purpose of thermoregulation, in addition to metabolic support of epidermal growth, given regular skin sloughing and nutrient

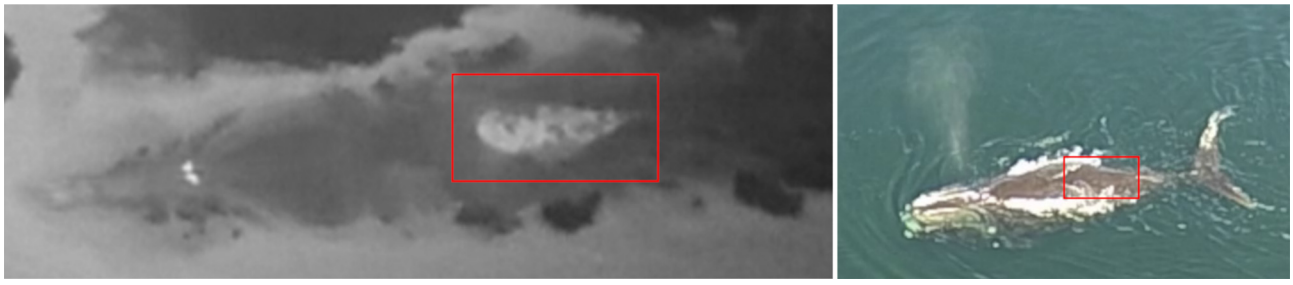

Fig. 10. Time-aligned video frames from the Zenmuse XT (left, white-hot color palette) and GoPro Hero3 (right) illustrating heat from the dorsum of an adult female North Atlantic right whale (Catalog ID 2791), which was likely pregnant at the time this video was taken

transport to/from blubber energy stores (Giacometti 1967, Haldiman et al. 1985, Haldiman & Tarpley 1993, Reeb et al. 2007). We did not observe any vasculature typically associated with countercurrent heat exchange or AVAs in the peri-callosity epithelium, suggesting that superficial blood vessels are not responsible for the adjacent epithelium being particularly warmer than the callosities. We acknowledge, however, that the one specimen we examined had been frozen and thawed before sampling for histology, potentially affecting the quality of histological slides. Otherwise, stiff hairs and hair follicles that are sparsely distributed in and around larger callosities and are associated with subdermal blood sinuses (Reeb et al. 2007) could be responsible for some peri-callosity heat.

We investigated an alternative hypothesis that exposure to sun and air during prolonged skim-feeding at the water surface could cause the peri-callosity epithelium to increase in temperature faster than the keratinized callosities. The warming study, however, demonstrated that both callosities and adjacent epithelial tissue had a similar thermal inertia between ~9 and 20°C in the laboratory (Fig. 7). The results of this study, the patchiness of heat patterns even on overcast days, and the presence of heat as soon as whales surface imply that peri-callosity heat is not due to differential exposure of the rostrum to water, sun, or air.

Instead, we suggest that the source of peri-callosity heat is subcutaneous, and that differences in the structure, conductive properties, and/or emissivity of the rostral integument are likely responsible for the unique patterns of cranial heat loss in NARWs. Specifically, we propose that the corpus cavernosum maxillaris could be the primary source of heat. First described by Ford and colleagues (2013) in the bowhead whale, the corpus cavernosum maxillaris is a highly vascularized retial organ that runs along the center of the hard palette of the upper mouth from the pterygoids to the tip of the rostrum, where it terminates in 2 large lobes (see Fig. 1 in Ford et al. 2013). Its main function is likely thermoregulation; during feeding, heat dissipates from the open mouth to the surrounding water, thereby protecting the brain from hyperthermia. In the context of our thermographs, heat from the corpus cavernosum maxillaris may conduct dorsally, thereby warming rostral tissue. Gross necropsy examinations of NARWs consistently show the hypodermis of the dorsal head to be thinner, more fibrous, and less oil-rich than postcranial blubber (M. Moore, pers. obs.), suggesting that the cranial hypodermis is less insulative in this region compared to the rest of the body because of its structural role. Meanwhile, the keratinized callosities of NARWs — with their thicker epidermis (Table 3) — may conduct less heat than the surrounding epidermis. Also, cyamids and water pooling in the crevices of the callosities could cause the surface of the callosities to appear cooler than the epithelium of the rest of the rostrum. This hypothesis is supported by thermographic images of the rostra of other species, namely humpback whales, which lack callosities and exhibit a more uniform heat signature across their dorsal heads (G. Lonati, unpubl. data). A subcutaneous heat source would also explain why these rostral heat patterns were visible even on a whale's first surfacing from depth.

Alternatively, the cranial tissues of NARWs might all exhibit similar temperatures but have variable emissivities. Emissivity is a physical property of an object and is generally defined as the efficiency with which an object radiates heat. Tissues with lower emissivities will appear cooler via IRT, even though they may be at the same temperature as tissues with higher emissivities (reviewed in Tattersall 2016). Emissivity, as well as reflected radiation, can also vary with the angle of the object relative to the IRT sensor (Jiao et al. 2016, Playà-Montmany & Tattersall 2021). Due to the curved, 3-dimensional shape of a whale's head, some parts of the rostrum might be observed at angles >30°, even when the RPAS and IRT camera are directly overhead the whale. This would increase reflected radiation, thereby decreasing emissivity (Ash et al. 1987, Tattersall 2016, Playà-Montmany & Tattersall 2021) and possibly producing a heterogeneous heat signature across the head. We must also acknowledge that a thin film of water over the whale's skin could reduce the amount of radiated heat the IRT sensor measures (Lathlean & Seuront 2014). However, the notable consistency of peri-callosity heat observed within and across individuals, even when a whale turned and as soon as a whale surfaced, suggests that this pattern is not an artifact of viewing angle or water masking heat from certain parts of the skin. Regardless, future work should investigate the emissivity of cetacean tissues (wet and dry) observed at various angles, with animals in managed care or necropsy specimens, using procedures outlined in Lathlean & Seuront (2014), for example.

In regard to the thermal anomalies observed at the tips of the rostra of some NARWs (Fig. 5), we propose 2 potential heat sources. One is the terminal lobes of the corpus cavernosum maxillaris (Ford et al. 2013). The other is the patch of hairs present in this region. NARWs have an array of approximately 300 small

hairs at the front of the head on the upper and lower jaw, with the highest concentration at the tip of the rostrum (Kenney et al. 2001, Murphy et al. 2022). These structures are considered to be vibrissae, or sensory hairs, and may facilitate prey detection or discrimination (Reeb et al. 2007). Vibrissae are known to have a subdermal follicle and dedicated blood supply. While there has been no histological investigation of the subdermal hair follicle in NARWs, it is presumed to be anatomically similar to the closely related bowhead whale (Drake et al. 2015) and to possess substantial innervation and vascularization. This blood flow to the individual follicles concentrated at the rostrum could collectively heat the area above the surrounding skin temperature. It is well established in the vibrissal literature on seals, otters, and some dolphins that the follicles appear significantly hotter than the surrounding skin areas using close-range IRT (e.g. Dehnhardt et al. 1998, Mauck et al. 2000, Kuhn & Meyer 2009, Erdsack et al. 2014). Based on evidence from these other species, it can be speculated that the dense array of sensory hairs in NARWs could represent a site of thermal radiation, appearing collectively when imaged from a distance as a hot spot in thermographs.

Understanding the sources of peri-callosity heat in NARWs and how they typically manifest in the unique heat signatures observed in RPAS-based thermographs could assist with monitoring injuries and entanglements and, as such, be a powerful tool to aid in the conservation of this species. More specifically, fishing gear can easily become wrapped around a NARW's rostrum and through the baleen, causing severe pain, inflammation, and tissue damage (Moore et al. 2006). This would result in increased blood flow to the area, thereby increasing the temperature of these tissues and changing the thermal signature that would be detected by RPAS-based IRT (Knížková et al. 2007, McCafferty 2007, Rekant et al. 2016). Thus, this technology has the important potential to document the severity of cranial entanglement injuries, monitor the healing process, and aid in rescue intervention decisions without causing further distress to the animal.

4.2. Thermal flukeprints

The thermal contrast of whale flukeprints is likely influenced by temperature profiles in the upper ~5 m of the water column, where the whales are skim-feeding and traveling subsurface. When there is strong solar radiation, calm winds (≤10 knots), and little mixing of the water column, the surface layer of water warms relative to subsurface water, establishing a shallow thermocline. Based on Fig. 9, we speculate that a shallow thermocline with a temperature differential of approximately 1°C is enough to observe and track thermal flukeprints produced by NARW upstrokes with our RPAS and IRT camera. However, the stability of these shallow thermoclines depends on currents and weather events, which vary on small spatial and temporal scales. Without finer resolution temperature data, it is difficult to explain the variable thermal contrast of whale flukeprints across all our field days. To elucidate the optimal conditions for observing thermal flukeprints and tracking NARWs with IRT, future work should record more detailed information on local weather conditions and collect water temperature profiles shortly before or after RPAS flights. Measurements of the length, duration, and size of thermal flukeprints could also inform future RPAS flight logistics (such as optimal altitude) and provide insight into swimming energetics and habitat use.

Previous studies have highlighted the usefulness of thermal flukeprints for detecting cetaceans during aerial surveys using IRT from human-occupied aircraft. For example, thermal flukeprints of humpback whales near Kodiak Island, AK, USA, were most visible when winds were <10 knots. Some flukeprints persisted for as long as 2 min and extended as far horizontally as 300 m (Churnside et al. 2009). Florko et al. (2021) detected thermal flukeprints from narwhals *Monodon monoceros* when the flukeprints were only 0.3–1.1°C warmer than the surrounding surface water. Our study further supports the use of aerial IRT to detect whales under certain oceanographic and meteorological conditions, even in a lower latitude habitat such as Cape Cod Bay. Considering the large, dedicated investment in aerial surveillance of NARWs in this region, IRT could increase the efficacy of NARW surveys to improve management efforts.

The thermal contrast of whales versus their surrounding aquatic environment can be harnessed for other avenues of research and conservation. For instance, IRT is already being tested and implemented for the automated oblique detection of whales and their blows to mitigate vessel collisions and acoustic disturbance (Yonehara et al. 2012, Zitterbart et al. 2013, 2020). The advantage of this technology is that it can be used during low-light conditions and nighttime, although detections are subject to other environmental conditions, particularly fog. In addition, aerial IRT could supplement visual tracking of NARWs during rescue interventions (both

through detecting hot blows or cool flukeprints), although both rescue and RPAS operations would also be hindered by fog and low-light conditions. Finally, RPAS-based IRT of flukeprints as well as the cold-water anomalies associated with the gapes of skim-feeding NARWs could be used to study the hydrodynamics of locomotion (Levy et al. 2011) and baleen filtration (Werth et al. 2019), respectively. For the latter phenomenon, subsurface skim-feeding likely draws colder, deeper water up to the surface, providing some insight about intra-oral water circulation (Video S2). In turn, thermographs of the water around whales with entanglements (during low sea states) may illustrate how hydrodynamics are interrupted by the presence of gear in the mouth or around the flippers and flukes.

4.3. Interpretations of post-cranial heat anomalies

During our fieldwork, we observed one whale with an anomalous heat signature on its dorsum, which was persistent over multiple surfacings (Fig. 10, Video S1), suggesting it was the result of underlying physiology and not a physical IRT artifact. While it is difficult to pinpoint the source of this heat with certainty, we can suggest a couple of explanations. First, underlying pathology or injury can result in inflammation that causes increased heat to exude from localized regions of the body (Knížková et al. 2007, McCafferty 2007, Rekant et al. 2016). The RGB imagery of the dorsum did not reveal any obvious external signs of injury (although the resolution was low), and the whale's body condition did not suggest that it was compromised or suffering from chronic injury or disease. That said, sublethal injuries from entanglements or vessel collisions are common in NARWs (Moore et al. 2021), so it is possible that this whale suffered a recent injury to its dorsum, such as blunt vessel trauma, that caused internal swelling or bruising. Another possibility is that the dorsal heat signature was related to the whale's pregnancy. This NARW was photo-identified as an adult female that was seen with a newborn calf 8 mo later (gestation in *Eubalaena* lasts approximately 12 mo; Best 1994). Pregnant NARWs are thought to have the thickest blubber layers of all age and sex classes (Miller et al. 2011) as well as increased drag due to a larger abdominal girth (McGregor 2010). While exerting itself during surface skim-feeding on a warm day, the pregnant NARW we observed might have been more prone to overheating, and the dorsal heat anomaly could have resulted from superficial vasodilation to dissipate excess heat. Other species of cetaceans are known to dissipate heat from their dorsal fins, particularly during exertion and/or exercise (Hampton & Whittow 1976, Noren et al. 1999, Williams et al. 1999, Meagher et al. 2002, Pabst et al. 2002, Barbieri et al. 2009, Horton et al. 2019), and while NARWs lack dorsal fins, perhaps the dorsal lumbar area is still an important thermal window for thermoregulation in this species.

For at-risk marine mammals such as the NARW, developing novel, non-invasive methods to conduct more thorough health assessments of individuals in response to multiple stressors is critical for species conservation. Researchers are beginning to recognize the value of IRT for health assessments of wild animals in addition to captive animals and livestock, where marked increases in the surface temperature of specific body parts can indicate disease or injury (reviewed in Hilsberg-Merz 2008, Cilulko et al. 2013). For example, studies have demonstrated that abnormal or asymmetrical heat signatures correspond with rabies in raccoons *Procyon lotor*, mange in wolves *Canis lupus*, changes in peripheral blood flow due to research tag attachment in grey seals *Halichoerus grypus*, and late-stage pregnancy in black rhinoceroses *Diceros bicornis* (Dunbar & MacCarthy 2006, McCafferty et al. 2007, Hilsberg-Merz 2008, Paterson et al. 2011, Cross et al. 2016). Pathologies could be similarly detected by looking for anomalous heat signatures from whales, although it is essential to first establish what a nonpathological heat signature looks like, while also acknowledging the limitations of IRT technology and difficulties associated with observing free-swimming whales above the water surface. At this time, a larger sample size of species, ages, and sexes would be helpful to better evaluate the physiological processes responsible for anomalous dorsal heat signatures, particularly in reproductive females, and confirm they are not a by-product of viewing angle or other physical IRT phenomenon. Ultimately, the ability to diagnose injuries or disease in real- or near-real-time could be of particular use to those studying NARWs or other at-risk marine mammal species. Since NARWs are often struck by vessels or entangled in fishing gear, this technology could eventually become an effective tool for quantifying sublethal injuries and monitoring compromised animals.

4.4. Future potential uses and considerations

Our study reviews 3 applications of RPAS-based IRT to collect qualitative data to study the thermal

physiology of free-ranging large whales. While the description of heat patterns and anomalies can prove useful for the reasons detailed above, one obvious next step is to measure absolute temperatures and quantify observed anomalies. However, collecting quantitative data via aerial IRT poses myriad challenges, particularly in aquatic environments.

First, it is important to understand the physical principles behind IRT, as well as its limitations. For instance, range and incident angle between the sensor and the target, atmospheric conditions (e.g. relative humidity, wind speed, and solar radiation), camera resolution, lens properties, emissivity, and reflection of long-wave infrared radiation from non-target sources can all influence the accuracy of IRT-derived temperature measurements (Cilulko et al. 2013, Lathlean & Seuront 2014, Faye et al. 2016, Tattersall 2016, Burke et al. 2019, Kelly et al. 2019, Playà-Montmany & Tattersall 2021). While these variables may not introduce significant errors when observing animals in managed care settings (Nienaber et al. 2010), their impact on IRT measurements in the field should be carefully considered. Furthermore, there is considerable variation in accuracy and precision among combinations of thermal sensor models and lenses, and thermal sensors can experience drifts in radiance response under different conditions (Olbrycht & Więcek 2015, Kelly et al. 2019, Playà-Montmany & Tattersall 2021). There exist several detailed reviews on these sources of error, including suggestions on how to account for them (McCafferty 2007, Lathlean & Seuront 2014, McCafferty et al. 2015, Faye et al. 2016, Tattersall 2016, Maes et al. 2017, Kelly et al. 2019, Playà-Montmany & Tattersall 2021).

Despite all these considerations, future studies that include thermal reference points, fly at low altitudes, incorporate sensor calibration protocols, and account for environmental variability could provide new, important health metrics of whales. For example, RPAS-based IRT of open whale blowholes could facilitate measurements of near-core temperatures, as previously described for captive bottlenose dolphins and beluga whales (Melero et al. 2015). Newer models of thermal sensors (e.g. the DJI Zenmuse XT2) are now capable of capturing radiometric video with simultaneous RGB video, which would preclude the need to synchronize radiometric still images with the opening of blowholes and would allow for the analysis of temperatures over the entire respiratory cycle (I. Kerr, Ocean Alliance, unpubl. data).

Based on the results of the present study, previously published research using new technologies to observe large whales, and the potential for quantitative temperature data collection, RPAS equipped with IRT and RGB cameras could theoretically diagnose pathologies or pregnancies, evaluate body condition via photogrammetry (Durban et al. 2015, 2016, Dawson et al. 2017, Christiansen et al. 2019, 2020), estimate heart rate (Horton et al. 2019), and measure body temperature in one whale encounter with minimal invasiveness. This significantly increases the scope and efficiency with which we can study and monitor the health of individual free-swimming whales in the face of multiple stressors. The above list is certainly not exhaustive and will only continue to grow with further advancements in technology and imagination. The faster these technologies can be developed and routinely and safely implemented, the sooner we can observe more NARWs, establish nonpathological baselines, and predict how trends in individual health will affect overall population-level health metrics, such as mortality and reproduction rates. This will vastly improve our ability to evaluate conservation success of management decisions.

5. CONCLUSIONS

Marine mammalogists should consider adding RPAS and IRT to their toolkits, especially those looking to collect novel, non-invasive health metrics on rare, Critically Endangered species, such as the NARW. We have shown how this emerging technology can be used to investigate the thermal physiology of large whales, monitor their health, and track them during at-sea operations. By first observing a range of nonpathological heat signatures from whales, we will be better poised to identify and interpret anomalous signatures that result from disease or injury. This will improve evaluations of sublethal trauma, the efficacy of rescue interventions, our understanding of population-level health, and future management decisions, especially for species that are subject to pervasive anthropogenic stressors. While there are physical limitations with IRT and challenges associated with operating and collecting measurements with the current technology in aquatic environments, these challenges can be circumvented with proper calibrations of the equipment and further research. Meanwhile, qualitative observations are already of real value for conservation.

Data accessibility. The following data produced during this study are publicly accessible through the Woods Hole Open Access Server (https://hdl.handle.net/1912/27049, doi:10.26025/1912/27049): (1) RGB and IRT imagery collected during RPAS flights, including raw videos from the Supple-

ment; (2) an imagery log summarizing all the imagery data files; and (3) a script to produce the generalized linear model for the warming study in R.

Acknowledgements. All activities were conducted under NOAA permit 18355-01 and were approved by Woods Hole Oceanographic Institution's Institutional Animal Care and Use Committee (IACUC). The RPAS pilot-in-command was certified through the United States Federal Aviation Administration. We thank Amy Knowlton (Anderson Cabot Center for Ocean Life at the New England Aquarium) for photo-identifying individual North Atlantic right whales and Rocky Geyer (Woods Hole Oceanographic Institution) for providing and interpreting water temperature data related to the observations of thermal flukeprints (courtesy of the Massachusetts Water Resources Authority). We also appreciate constructive conversations with Iain Kerr (Ocean Alliance), Chris Zadra (Ocean Alliance), and Joy Reidenberg (Icahn School of Medicine at Mount Sinai). Funding was provided by a Woods Hole Oceanographic Research Opportunity grant, the North Pond Foundation, and NMFS NA14OAR4320158.

LITERATURE CITED

Ash CJ, Gotti E, Haik CH (1987) Thermography of the curved living skin surface. Miss Med 84:702–708

Austin D, Bowen WD, Mcmillan JI, Boness DJ (2006) Stomach temperature telemetry reveals temporal patterns of foraging success in a free-ranging marine mammal: temporal distribution of feeding in grey seals. J Anim Ecol 75:408–420

Barbieri MM, McLellan WA, Wells RS, Blum JE, Hofmann S, Gannon J, Pabst DA (2009) Using infrared thermography to assess seasonal trends in dorsal fin surface temperatures of free-swimming bottlenose dolphins (*Tursiops truncatus*) in Sarasota Bay, Florida. Mar Mamm Sci 26: 53–66

Best PB (1994) Seasonality of reproduction and the length of gestation in southern right whales *Eubalaena australis.* J Zool 232:175–189

Burke C, Rashman M, Wich S, Symons A, Theron C, Longmore S (2019) Optimizing observing strategies for monitoring animals using drone-mounted thermal infrared cameras. Int J Remote Sens 40:439–467

Christiansen F, Sironi M, Moore MJ, Di Martino M and others (2019) Estimating body mass of free-living whales using aerial photogrammetry and 3D volumetrics. Methods Ecol Evol 10:2034–2044

Christiansen F, Dawson SM, Durban JW, Fearnbach H and others (2020) Population comparison of right whale body condition reveals poor state of the North Atlantic right whale. Mar Ecol Prog Ser 640:1–16

Churnside J, Ostrovsky L, Veenstra T (2009) Thermal footprints of whales. Oceanogr 22:206–209

Cilulko J, Janiszewski P, Bogdaszewski M, Szczygielska E (2013) Infrared thermal imaging in studies of wild animals. Eur J Wildl Res 59:17–23

Codde SA, Allen SG, Houser DS, Crocker DE (2016) Effects of environmental variables on surface temperature of breeding adult female northern elephant seals, *Mirounga angustirostris*, and pups. J Therm Biol 61:98–105

Cooke JG (2020) *Eubalaena glacialis* (errata version published in 2020). The IUCN Red List of Threatened Species e.T41712A178589687. https://dx.doi.org/10.2305/IUCN.UK.2020-2.RLTS.T41712A178589687.en

Cross PC, Almberg ES, Haase CG, Hudson PJ and others (2016) Energetic costs of mange in wolves estimated from infrared thermography. Ecology 97:1938–1948

Cutchis PN, Hogrefe AF, Lesho JC (1988) The ingestible thermal monitoring system. Johns Hopkins APL Tech Dig 9:16–21

Cuyler LC, Wiulsrod R, Oritsland NA (1992) Thermal infrared radiation from free living whales. Mar Mamm Sci 8:120–134

Davies KTA, Brillant SW (2019) Mass human-caused mortality spurs federal action to protect endangered North Atlantic right whales in Canada. Mar Policy 104:157–162

Dawson SM, Bowman MH, Leunissen E, Sirguey P (2017) Inexpensive aerial photogrammetry for studies of whales and large marine animals. Front Mar Sci 4:366

Dehnhardt G, Mauck B, Hyvärinen H (1998) Ambient temperature does not affect the tactile sensitivity of mystacial vibrissae in harbour seals. J Exp Biol 201:3023–3029

Drake SE, Crish SD, George JC, Stimmelmayr R, Thewissen JGM (2015) Sensory hairs in the bowhead whale, *Balaena mysticetus* (Cetacea, Mammalia). Anat Rec 298: 1327–1335

Dunbar MR, MacCarthy KA (2006) Use of infrared thermography to detect signs of rabies infection in raccoons (*Procyon lotor*). J Zoo Wildl Med 37:518–523

Durban JW, Fearnbach H, Barrett-Lennard LG, Perryman WL, Leroi DJ (2015) Photogrammetry of killer whales using a small hexacopter launched at sea. J Unmanned Veh Syst 3:131–135

Durban JW, Moore MJ, Chiang G, Hickmott LS and others (2016) Photogrammetry of blue whales with an unmanned hexacopter. Mar Mamm Sci 32:1510–1515

Elsner R, George JC, O'Hara T (2004) Vasomotor responses of isolated peripheral blood vessels from bowhead whales: thermoregulatory implications. Mar Mamm Sci 20:546–553

Erdsack N, Hanke FD, Dehnhardt G, Hanke W (2012) Control and amount of heat dissipation through thermal windows in harbor seals (*Phoca vitulina*). J Therm Biol 37: 537–544

Erdsack N, Dehnhardt G, Hanke W (2014) Thermoregulation of the vibrissal system in harbor seals (*Phoca vitulina*) and Cape fur seals (*Arctocephalus pusillus pusillus*). J Exp Mar Biol Ecol 452:111–118

Faye E, Dangles O, Pincebourde S (2016) Distance makes the difference in thermography for ecological studies. J Therm Biol 56:1–9

Florko KRN, Carlyle CG, Young BG, Yurkowski DJ, Michel C, Ferguson SH (2021) Narwhal (*Monodon monoceros*) detection by infrared flukeprints from aerial survey imagery. Ecosphere 12:e03698

Ford TJ, Werth AJ, George JC (2013) An intraoral thermoregulatory organ in the bowhead whale (*Balaena mysticetus*), the corpus cavernosum maxillaris. Anat Rec 296:701–708

Giacometti L (1967) The skin of the whale (*Balaenoptera physalus*). Anat Rec 159:69–75

Guerrero AI, Rogers TL, Sepúlveda M (2021) Conditions influencing the appearance of thermal windows and the distribution of surface temperature in hauled-out southern elephant seals. Conserv Physiol 9:coaa141

Haldiman JT, Tarpley R (1993) Anatomy and physiology. In: Lawrence KS (ed) The bowhead whale. Special Publica-

tion 2. The Society for Marine Mammalogy, Allen Press, New York, NY, p 71–156
Haldiman JT, Henk WG, Henry RW, Albert TF, Abdelbaki YZ, Duffield DW (1985) Epidermal and papillary dermal characteristics of the bowhead whale (*Balaena mysticetus*). Anat Rec 211:391–402
Hampton IFG, Whittow GC (1976) Body temperature and heat exchange in the Hawaiian spinner dolphin, *Stenella longirostris*. Comp Biochem Physiol A Physiol 55:195–197
Harcourt R, van der Hoop J, Kraus S, Carroll EL (2019) Future directions in *Eubalaena* spp.: comparative research to inform conservation. Front Mar Sci 5:530
Heyning JE (2001) Thermoregulation in feeding baleen whales: morphological and physiological evidence. Aquat Mamm 27:284–288
Hilsberg-Merz S (2008) Infrared thermography in zoo and wild animals. In: Fowler ME, Miller RE (eds) Zoo and wild animal medicine current therapy, Vol 6. Saunders, Elsevier, St Louis, MO, p 20–32
Horton TW, Oline A, Hauser N, Khan TM and others (2017) Thermal imaging and biometrical thermography of humpback whales. Front Mar Sci 4:424
Horton TW, Hauser N, Cassel S, Klaus KF, Fettermann T, Key N (2019) Doctor drone: non-invasive measurement of humpback whale vital signs using unoccupied aerial system infrared thermography. Front Mar Sci 6:466
Jiao L, Dong D, Zhao X, Han P (2016) Compensation method for the influence of angle of view on animal temperature measurement using thermal imaging camera combined with depth image. J Therm Biol 62:15–19
Johnston DW, Dale J, Murray K, Josephson E, Newton E, Wood S (2017) Comparing occupied and unoccupied aircraft surveys of wildlife populations: assessing the gray seal (*Halichoerus grypus*) breeding colony on Muskeget Island, USA. J Unmanned Veh Syst 5:178–191
Katsumata E, Jaroenporn S, Katsumata H, Konno S, Maeda Y, Watanabe G, Taya K (2006) Body temperature and circulating progesterone levels before and after parturition in killer whales (*Orcinus orca*). J Reprod Dev 52:65–71
Kelly J, Kljun N, Olsson PO, Mihai L and others (2019) Challenges and best practices for deriving temperature data from an uncalibrated UAV thermal infrared camera. Remote Sens 11:567
Kenney RD, Mayo CA, Winn HE (2001) Migration and foraging strategies at varying spatial scales in western North Atlantic right whales: a review of hypotheses. J Cetacean Res Manag 2:251–260
Knížková I, Kunc P, Ka GA (2007) Applications of infrared thermography in animal production. J Fac Agric OMU 22:329–336
Knowlton AR, Kraus SD (2001) Mortality and serious injury of northern right whales (*Eubalaena glacialis*) in the western North Atlantic Ocean. J Cetacean Res Manag 2: 193–208
Kuhn RA, Meyer W (2009) Infrared thermography of the body surface in the Eurasian otter *Lutra lutra* and the giant otter *Pteronura brasiliensis*. Aquat Biol 6:143–152
Lathlean J, Seuront L (2014) Infrared thermography in marine ecology: methods, previous applications and future challenges. Mar Ecol Prog Ser 514:263–277
Levy R, Uminsky D, Park A, Calambokidis J (2011) A theory for the hydrodynamic origin of whale flukeprints. Int J Non-linear Mech 46:616–626
Lydersen C, Chernook VI, Glazov DM, Trukhanova IS, Kovacs KM (2012) Aerial survey of Atlantic walruses (*Odobenus rosmarus rosmarus*) in the Pechora Sea, August 2011. Polar Biol 35:1555–1562
Mackay RS (1964) Deep body temperature of untethered dolphin recorded by ingested radio transmitter. Science 144:864–866
Maes W, Huete A, Steppe K (2017) Optimizing the processing of UAV-based thermal imagery. Remote Sens 9: 476
Martony ME, Isaza R, Erlacher-Reid CD, Peterson J, Stacy NI (2020) Esophageal measurement of core body temperature in the Florida manatee (*Trichechus manatus latirostris*). J Wildl Dis 56:27–33
Mauck B, Eysel U, Dehnhardt G (2000) Selective heating of vibrissal follicles in seals (*Phoca vitulina*) and dolphins (*Sotalia fluviatilis guianensis*). J Exp Biol 203: 2125–2131
Mauck B, Bilgmann K, Jones DD, Eysel U, Dehnhardt G (2003) Thermal windows on the trunk of hauled-out seals: hot spots for thermoregulatory evaporation? J Exp Biol 206:1727–1738
McCafferty DJ (2007) The value of infrared thermography for research on mammals: previous applications and future directions. Mammal Rev 37:207–223
McCafferty DJ, Currie J, Sparling CE (2007) The effect of instrument attachment on the surface temperature of juvenile grey seals (*Halichoerus grypus*) as measured by infrared thermography. Deep Sea Res II 54:424–436
McCafferty DJ, Gallon S, Nord A (2015) Challenges of measuring body temperatures of free-ranging birds and mammals. Anim Biotelem 3:33
McGregor AEN (2010) The cost of locomotion in North Atlantic right whales *Eubalaena glacialis*. PhD dissertation, Duke University, Durham, NC
Meagher EM, McLellan WA, Westgate AJ, Wells RS, Frierson D Jr, Pabst DA (2002) The relationship between heat flow and vasculature in the dorsal fin of wild bottlenose dolphins, *Tursiops truncatus*. J Exp Biol 205:3475–3486
Melero M, Rodríguez-Prieto V, Rubio-García A, García-Párraga D, Sánchez-Vizcaíno JM (2015) Thermal reference points as an index for monitoring body temperature in marine mammals. BMC Res Notes 8:411
Meyer-Gutbrod EL, Greene CH, Sullivan PJ, Pershing AJ (2015) Climate-associated changes in prey availability drive reproductive dynamics of the North Atlantic right whale population. Mar Ecol Prog Ser 535:243–258
Meyer-Gutbrod EL, Greene CH, Davies KTA, Johns DG (2021) Ocean regime shift is driving collapse of the North Atlantic right whale population. Oceanography 34:23–31
Miller CA, Reeb D, Best PB, Knowlton AR, Brown MW, Moore MJ (2011) Blubber thickness in right whales *Eubalaena glacialis* and *Eubalaena australis* related with reproduction, life history status and prey abundance. Mar Ecol Prog Ser 438:267–283
Moore M, Bogomolni A, Bowman R, Hamilton P and others (2006) Fatally entangled right whales can die extremely slowly. In: OCEANS 2006. IEEE, Boston, MA. https://ieeexplore.ieee.org/document/4098947
Moore MJ, Rowles TK, Fauquier DA, Baker JD and others (2021) Assessing North Atlantic right whale health: threats, and development of tools critical for conservation of the species. Dis Aquat Org 143:205–226
Murphy CT, Marx M, Martin WN, Jiang H and others (2022) Feeling for food: Can rostro-mental hair arrays sense hydrodynamic cues for foraging North Atlantic right whales? Anat Rec 305:577–591

Nääs IA, Garcia RG, Caldara FR (2014) Infrared thermal image for assessing animal health and welfare. J Anim Behav Biometeorol 2:66–72

Nienaber J, Thomton J, Horning M, Polasek L, Mellish JA (2010) Surface temperature patterns in seals and sea lions: a validation of temporal and spatial consistency. J Therm Biol 35:435–440

Noren DP, Williams TM, Berry P, Butler E (1999) Thermoregulation during swimming and diving in bottlenose dolphins, *Tursiops truncatus*. J Comp Physiol B 169:93–99

Nowacek DP, Christiansen F, Bejder L, Goldbogen JA, Friedlaender AS (2016) Studying cetacean behaviour: new technological approaches and conservation applications. Anim Behav 120:235–244

Olbrycht R, Więcek B (2015) New approach to thermal drift correction in microbolometer thermal cameras. Quant Infrared Thermogr J 12:184–195

Pabst D, McLellan W, Fougeres E, Westgate A (2002) Measuring temperatures and heat flux from dolphins in the Eastern Tropical Pacific: Is thermal stress associated with chase and capture in the ETP-tuna purse seine fishery? Southwest Fisheries Science Center, La Jolla, CA

Paterson W, Pomeroy PP, Sparling CE, Moss S, Thompson D, Currie JI, McCafferty DJ (2011) Assessment of flipper tag site healing in gray seal pups using thermography. Mar Mamm Sci 27:295–305

Perryman WL, Donahue MA, Laake JL, Martin TE (1999) Diel variation in migration rates of Eastern Pacific gray whales measured with thermal imaging sensors. Mar Mamm Sci 15:426–445

Pettis HM, Pace RM III, Hamilton PK (2022) North Atlantic Right Whale Consortium 2021 Annual Report Card. Report to the North Atlantic Right Whale Consortium. https://www.narwc.org/uploads/1/1/6/6/116623219/2021report_cardfinal.pdf

Pirotta E, Booth CG, Costa DP, Fleishman E and others (2018) Understanding the population consequences of disturbance. Ecol Evol 8:9934–9946

Pirotta E, Thomas L, Costa DP, Hall AJ and others (2022) Understanding the combined effects of multiple stressors: a new perspective on a longstanding challenge. Sci Total Environ 821:153322

Playà-Montmany N, Tattersall GJ (2021) Spot size, distance, and emissivity errors in field applications of infrared thermography. Methods Ecol Evol 12:828–840

R Core Team (2021) R: a language and environment for statistical computing. R Foundation for Statistical Computing, Vienna. https://www.R-project.org/

Record N, Runge J, Pendleton D, Balch W and others (2019) Rapid climate-driven circulation changes threaten conservation of endangered North Atlantic right whales. Oceanography 32:162–169

Reeb D, Best PB, Kidson SH (2007) Structure of the integument of southern right whales, *Eubalaena australis*. Anat Rec 290:596–613

Rekant SI, Lyons MA, Pacheco JM, Arzt J, Rodriguez LL (2016) Veterinary applications of infrared thermography. Am J Vet Res 77:98–107

Rolland RM, Schick RS, Pettis HM, Knowlton AR, Hamilton PK, Clark JS, Kraus SD (2016) Health of North Atlantic right whales *Eubalaena glacialis* over three decades: from individual health to demographic and population health trends. Mar Ecol Prog Ser 542:265–282

Seymour AC, Dale J, Hammill M, Halpin PN, Johnston DW (2017) Automated detection and enumeration of marine wildlife using unmanned aircraft systems (UAS) and thermal imagery. Sci Rep 7:45127

Sharp SM, McLellan WA, Rotstein DS, Costidis AM and others (2019) Gross and histopathologic diagnoses from North Atlantic right whale *Eubalaena glacialis* mortalities between 2003 and 2018. Dis Aquat Org 135:1–31

Tattersall GJ (2016) Infrared thermography: a non-invasive window into thermal physiology. Comp Biochem Physiol A Mol Integr Physiol 202:78–98

Thomas GL, Thorne RE (2001) Night-time predation by Steller sea lions. Nature 411:1013

Werth AJ, Kosma MM, Chenoweth EM, Straley JM (2019) New views of humpback whale flow dynamics and oral morphology during prey engulfment. Mar Mamm Sci 35: 1556–1578

Westgate AJ, McLellan WA, Wells RS, Scott MD, Meagher EM, Pabst DA (2007) A new device to remotely measure heat flux and skin temperature from free-swimming dolphins. J Exp Mar Biol Ecol 346:45–59

Williams TM, Noren D, Berry P, Estes JA, Allison C, Kirtland J (1999) Thermoregulation in diving dolphins. J Exp Biol 202:2763–2769

Yonehara Y, Kagami L, Yamada H, Kato H, Terada M, Okada S (2012) Feasibility of infrared detection of cetaceans for avoiding collision with hydrofoil. Int J Mar Nav Safety Sea Transport 6:149–154

York G, Amstrup S, Simac K (2004) Using forward looking infrared (FLIR) imagery to detect polar bear materal dens. US Department of the Interior, Anchorage, AK

Young BG, Yurkowski DJ, Dunn JB, Ferguson SH (2019) Comparing infrared imagery to traditional methods for estimating ringed seal density. Wildl Soc Bull 43:121–130

Zitterbart DP, Kindermann L, Burkhardt E, Boebel O (2013) Automatic round-the-clock detection of whales for mitigation from underwater noise impacts. PLOS ONE 8: e71217

Zitterbart DP, Smith HR, Flau M, Richter S and others (2020) Scaling the laws of thermal imaging-based whale detection. J Atmos Ocean Technol 37:807–824

Editorial responsibility: Aaron N. Rice, Ithaca, New York, USA
Reviewed by T. Horton and 2 anonymous referees

Submitted: May 29, 2021
Accepted: May 2, 2022
Proofs received from author(s): June 27, 2022